Article

Atmospheric Contamination of Coastal Cities by the Exhaust Emissions of Docked Marine Vessels: the case of Tromsø

Asier Zubiaga [1]*0000-0001-6603-9336, Synne Madsen [2], Hassan Khawaja [2]0000-0002-0252-3476 and Gernot Boiger [1]0000-0001-5613-2465

[1] ZHAW, Inst. Computational Physics, Technikumstrasse 9, CH-8401 Winterthur (Switzerland)
[2] UiT The Arctic University of Norway, Tromsø, Norway
* Correspondence: asier.zubiaga@zhaw.ch
† Current address: asier.zubiaga@gmail.com

Abstract: Docked ships are a source of contamination for the city while they keep their engine working. Plumes emissions from large boats can carry a number of pollutants to the nearby cities causing a detrimental effect on the life quality and health of local citizens and ecosystems. A computational fluid dynamics model of the harbour area of Tromsø has been built in order to model the deposition of CO_2 gas emitted by docked vessels within the city. The ground level distribution of the emitted gas has been obtained and the influence of the wind speed and direction, vessel chimney height, ambient temperature and exhaust gas temperature has been studied. The deposition range is found to be the largest when the wind speed is low. At high wind speeds, the deposition of pollutants along the wind direction is enhanced and spots of high pollutant concentration can be created. The simulation model is intended for the detailed study of the contamination in cities near the coast or an industrial pollutant source of any type of gas pollutants and can easily be extended for the study of particulate matter.

Keywords: computational fluid dynamics; OpenFOAM; docked vessel; gas pollutants

1. Introduction

Plumes emissions from industrial activities and large boats can carry a number of pollutants to the nearby cities causing a detrimental effect on the life quality and health of local citizens and ecosystems [1,2]. The main pollutants are waste products of combustion processes, mainly carbon monoxide (CO), nitrogen and sulfur oxides (NO_x, SO_x) in gas phase and solid particulate matter. They are released as suspended particles in the exhaust gases. Carbon dioxide (CO_2) is the main by-product in exhaust plumes. Although it does not have a direct health effect, it is well-known its influence on the climate warming.

Docked ships are a source of contamination for the city while they keep their engine working [3–6]. The contamination of the city is related to the deposited fraction of particulates and gas traces at street level. The exhaust gas and the suspended particulates are transported by the wind over the habited areas [7,8]. The interplay between the wind and the local orography will determine the transport distance and the fraction reaching the ground level [9,10].

The pollutants can be divided into two types: gas molecules and larger particulate matter [11]. Each has different transport mechanisms. While gas pollutants are transported as part of the main fluid, solid particles are subject to the drag by the fluid and they tend to suspend by gravity. Both types of particles are emitted from an exhaust at a relatively large concentration and they mix and dilute thanks to the buoyancy effects and lateral diffusion. This last effect is specially important in the gas phase and it will increase the effective diffusion range of gas particles. On the other hand, particulate matter is mainly driven by the buoyancy and the drag forces. This has an effect on their distribution close to the emission point. An accurate assessment of the contaminant distributions can be achieved using real scale atmospheric simulations including the local terrain orography and building distribution. A real scale model should consider as input parameters the atmospheric condition (temperature, wind and pressure), the topography of the studied

Citation: Zubiaga, A.;Madsen, S. K. ; Khawaja, H. A.; Boiger, G. K. Atmospheric Contamination of a Coastal City by the Exhaust Emissions of Docked Marine Vessels: the case of Tromso. *Preprints* **2021**, *1*, 0. https://doi.org/

Received:
Accepted:
Published:

Preprints (www.preprints.org) | NOT PEER-REVIEWED | Posted: 4 August 2021 doi:10.20944/preprints202108.0113.v1

area and the position and size of the main buildings. To study the contamination coming from docked vessels, also the height of the exhaust and the temperature of the plume must also be considered.

In this work, we use computational fluid dynamics simulations of flowing air on a topographic model of the sea side in the city of Tromsø. The emission from docked vessels and the interplay between the general wind flow and the exhaust gas have been modelled in detail. Special attention has been given to the dispersion of a trace gas, CO_2 in this study, that is representative for the dispersion of pollutants emitted by the vessel and their distribution at street level. In Section 2, the used computational technique are described. The main results are given in Section 3 and the most important results are discussed in Section 4. Finally, the main conclusions are summarized in Section 5.

2. Materials and Methods

The study of the pollutant distribution is based in a computational fluid dynamics (CFD) simulation of the exhaust gas distribution over and within the city of Tromsø. The simulation is based in a topographic model of the harbour area of the city. The ground topographic model has a diameter of 800 m, shown in Figure 1, and describes the main buildings near the harbour area together with the main features of the terrain. The height of the ground model ranges between 0 m at the sea and 34 m at the highest point. The typical height of the buildings range between 5 m and 10 m. An air column of up to 300 m has been added for the fluid simulation. The resulting simulation domain has a cylindrical shape truncated below by the non flat terrain.

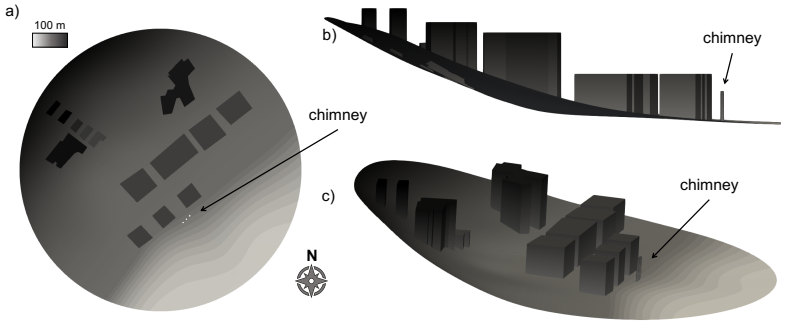

Figure 1. Topographic model of the harbour area of Tromsø. The a) vertical, b) lateral and c) oblique view of the topographic model is shown. The vertical scale has been magnified (×5) for clarity.

The emission of the vessel is described with a chimney of variable height, 5 m, 10 m and 20 m, in the harbour. For the temperatures of the emitted gas at the exit of the chimney values between 10°C and 200°C have been used. The exit speed of the exhaust gas has been set at 25 m/s, 40% of the emitted gas is CO_2 and the rest is air. The environment temperature has been varied between 0°C and 20°C.

2.1. Computational Fluid Dynamics

In CFD the air column is described with the Navier-Stokes equation with the gravitation $\vec{g}$ as an external force

$$\frac{\partial \vec{u}}{\partial t} + \left(\vec{u} \cdot \vec{\nabla}\right)\vec{u} = \nu \nabla^2 \vec{u} - \frac{\vec{\nabla} P}{\rho} + \vec{g}. \tag{1}$$

The magnitudes solved for are the fluid velocity $\vec{u}$ and the atmospheric pressure P. The fluid has a kinematic viscosity ν and its density is ρ. The gases are compressible and ρ is modified by the combined effect of the temperature T and pressure P. They are linked by the equation state of ideal gases

$$P = nRT. \tag{2}$$

Preprints (www.preprints.org) | NOT PEER-REVIEWED | Posted: 4 August 2021 doi:10.20944/preprints202108.0113.v1

R is the molar gas constant $\sim 8.315\ J/(Kmol)$ and n is the molar density. The total fluid density ρ and the fluid velocity $\vec{u}$ are linked by the mass transport equation

$$\frac{\partial \rho}{\partial t} + \vec{\nabla}(\rho \vec{u})\vec{u} = 0 \tag{3}$$

The atmosphere of Earth is composed of nitrogen (78%) and oxygen (21%) mainly. Several other gases appear at a lower concentration (noble gases argon, neon, helium and krypton, carbon dioxide CO_2 and methane NH_4 and water vapour). In this work, we are interested in the transport and diffusion of trace gases. For this purpose, we have separated the gas phase into two components. The main components describes dry air with a mass density of $1.2\ kg/m^3$ at sea level and a trace component expelled from the vessel exhaust. For the trace component CO_2 has been chosen throughout the work. Within the ideal gas approximation, the behaviour of the trace gas is representative of other gas phase pollutants also.

The wind velocities have defined as the wind speed and direction in the upper part of the simulation domain. The speed values considered for this work range between $1\ m/s$ and $15\ m/s$. Four directions have been considered starting from $\hat{u} = (-1, 1, 0)$ and varying the orientation of the direction vector by $90°$. The high Reynolds number $Re = uL/\nu \gg 1000$ corresponds to the turbulent regime. The $\kappa - \epsilon$ Reynolds Averaged Simulation (RAS) turbulence model [12] has been used to describe the turbulences.

2.2. Atmospheric boundary layer

The simulation of an atmospheric air column requires setting up carefully the boundary conditions of the circulating air. The wind flow along the computational domain has been stabilized using the atmospheric boundary layer model developed by Richards and Norris [13] with the generalized formulation used by Hargreaves et al. [14] and Yang et al. [15] . The velocity is fixed and horizontal in the atmospheric boundaries with a vertical profile

$$u_{ABL}(z) = \frac{U^*}{\kappa} \ln\left(\frac{z - z_g + z_0}{z_0}\right). \tag{4}$$

$\kappa = 0.41$ is the von Karman constant, z_g the topographic ground height, which value at each point depends on the topographic height, and z_0 a surface roughness coefficient that has been set up to $5\ m$ to match the buildings height. The friction velocity U^* is a reference value calculated as $U^* = \kappa u_{ref} / \ln((z_{ref} + z_0)/z_0)$. The velocity u_{ref} has been chosen equal to the wind speed in the upper limit of the simulation domain.

For the temperature of the air at sea level ($z \sim 0\ m$) $T_0 = 0°C$, $10°C$ and $20°C$ have been chosen. The temperature in the atmospheric lateral boundaries has been fixed to a linear profile $T = T_0 - 0.01z$. The turbulence model parameters are also set up as

$$k = \frac{U^{*2}}{\sqrt{C_\mu}} \tag{5}$$

$$\epsilon = \frac{U^{*3}}{\kappa(z - z_g - z_0)} \tag{6}$$

$C_\mu = 0.09$ being the turbulent viscosity coefficient.

2.3. Numerical solutions

The simulations have been run using the OpenFOAM [16] CFD software based in the field operation and manipulation (FOAM) C++ class library for continuum mechanics. OpenFOAM uses the finite volume numerical method to integrate the Navier-Stokes equation. A tetragonal finite element mesh of 1.3 millions cells has been used. The mesh has been refined around the main features of the terrain. The size of the mesh elements and the degree of refinement close to the main features are illustrated in Figure 2.

Preprints (www.preprints.org) | NOT PEER-REVIEWED | Posted: 4 August 2021 doi:10.20944/preprints202108.0113.v1

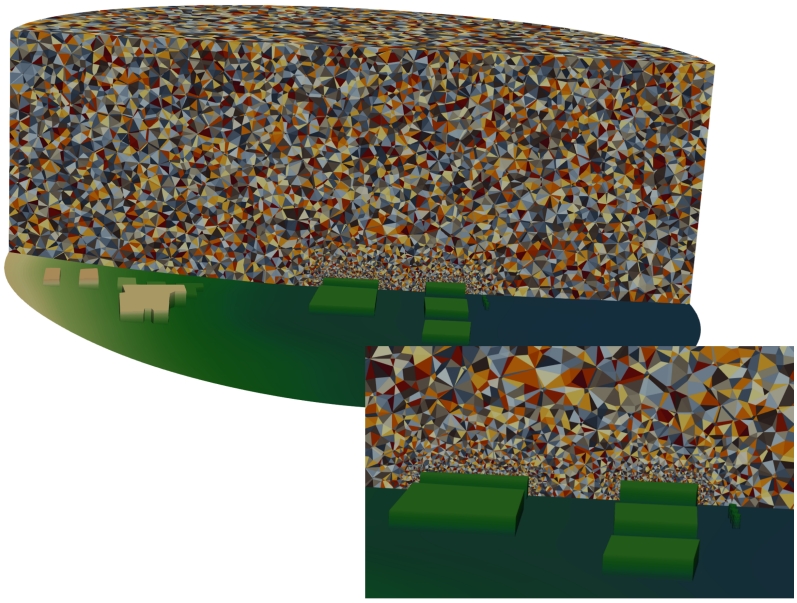

Figure 2. Tetrahedral mesh. Clip of the tetrahedral mesh used for the CFD simulation with OpenFOAM. The inset shows a detailed view of the finer mesh in the bottom boundary and near the terrain features.

The simulated gas mixture is composed by atmospheric air and a trace component, that in this simulation has been identified with CO_2. The trace gas is expelled by the docked vessel through its chimney. In the plume outlet, 40% of the outgoin gas mass corresponds to CO_2. The mixing of the gases is calculated at each time step using the mass conservation equation (Equation 3). Buoyancy effects are included and the thermodynamical model of the fluids takes includes the enthalpy h_f and the specific heat capacity c_p. The transport properties are described through the dynamic viscosity μ and the Prandtl number Pr. Their values for each component of the mixture are given in Table 1. The boundary conditions set for the simulations are listed in Table 2.

Table 1. Transport and thermodynamic parameters. All the values are given for 1 atm and 285 K.

	Air	CO_2	
Viscosity μ	17.9	13.7	$\mu Pa \cdot s$
Prandtl number Pr	0.71	0.765	–
Molar weight n	28.97	44.01	g/mol
Specific heat capacity c_p	1005	846	$J/(kg \cdot K)$
Enthalpy h_f	330	8647	J/kg

Equations 1-3 are solved using a combination of the PISO (Pressure-Implicit with Splitting of Operators) algorithm [17] and the SIMPLE (Semi-Implicit Method for Pressure Linked Equations) algorithm [18]. This choice allows to increase the size of the time step to speed up the simulation. The transient simulation is run for 1000 s simulation time in parallel in 32 cores. The long simulation time was chosen to ensure that the wind flow and the CO_2 distribution reaches a stationary state.

The study addreses the effect of the wind speeds and directions, the atmospheric temperature, the chimney height and the exhaust gas temperature. The wind speed and directions and the direction cover the most usual atmospheric conditions in the city of Tromsø. On the other hand, the chimney height and the exhaust gas temperature describe the most important variables of the exhaust emission. The values chosen for the parameter study are given in Table 3.

Preprints (www.preprints.org) | NOT PEER-REVIEWED | Posted: 4 August 2021 doi:10.20944/preprints202108.0113.v1

Table 2. Boundary conditions. All the boundary conditions used are detailed. The solver solves the quantity $P - \rho gz$ instead ofthe total atmospheric pressure. Its boundary value is set up so that the gradient matches the velocity boundary condition.

Boundary conditions	
$P - \rho(z)gz$	Fixed flux
ρ, Y_{CO_2}	Zero gradient
Top boundary	
$\vec{u}$	Fixed uniform (ABL)
k, ϵ, T	Zero gradient
Side boundaries	
$\vec{u}$, k, ϵ	Fixed non-uniform (ABL)
T	Fixed non-uniform ($-0.01\ K/m$)
Ground	
$\vec{u}$	Non-slip
T	Zero gradient
k, ϵ	Wall function
Exhaust	
$\vec{u}$	Fixed value ($25\ m/s\ \hat{z}$)
T	Total temperature
k	Turbulent intensity (0.05)
ϵ	Turbulent mixing length ($50\ m$)

Table 3. Simulation parameters. The parameters of the studies and their values are given. The highlighted values are the parameter values for the reference case.

Wind speed	u	$1, 3, \mathbf{5}, 15\ m/s$
Wind direction	$\hat{u}$	NW $(-\mathbf{1}, \mathbf{1}, \mathbf{0})$, NE $(1, 1, 0)$, SE $(1, -1, 0)$, SW $(-1, -1, 0)$
Ambient temperature	T_0	$0°, \mathbf{10}°, 20°\ C$
Chimney height	h_c	$5, \mathbf{10}, 20\ m$
Exhaust temperature	T_c	$10°, \mathbf{110}°, 200°\ C$

3. Results

The simulation of the atmospheric boundary layer possess a challenge for CFD. The main problem lies in the inherently turbulent nature of the atmospheric flow and the cloud formation, further complicated by the orography of the terrain and the buildings [19,20]. A realistic wind flow requires taking into account many details like the changes of the transport properties with temperature and pressure, as well as the boundary conditions in contact with the terrain or in the top of the simulation domain. The thermodynamical properties of the gas mixture composing the air has also to account for the heat transfer properties with diverse heat sources, the solar insolation or the content of water vapour.

When the simulation is performed for stable atmospheric conditions and it is constrained to the lower part of the atmospheric boundary layer, the surface layer, a stable wind flow can be obtained using a $k - \epsilon$ turbulence model [21] and setting the boundary conditions proposed by Richard and Hoxey [13] for the velocity, the pressure as well as the turbulent kinetic energy k and its dissipation rate ϵ.

Between the lower and the upper boundary of the simulation domain the thermodynamical quantities vary by only 3.5% for the pressure, 1% the temperature and 2.5% the molar density n of an ideal gas. The narrow thermodynamical conditions allow using a constant value of the transport and thermodynamic properties.

Contrarily, the simplifying assumption of incompressibility cannot be done for the atmospheric gas. The equation of state for the perfect gas has been used to connect the pressure to the thermodynamical properties of the fluid (Temperature, enthalpy and specific

Preprints (www.preprints.org) | NOT PEER-REVIEWED | Posted: 4 August 2021 doi:10.20944/preprints202108.0113.v1

heat capacity) as well as the mass density. The relevant parameters are given in Table 1. To ensure a stable run, an appropriate choice of the boundary conditions and the initial conditions is crucial. To constrain $\vec{U}$ and the turbulence model parameters (k, ϵ) in the lateral boundaries the ABL condition are used. The ABL values correspond to a stable dry atmosphere with a defined wind flow at heights well above the orographic obstacles. The temperature is constrained to be equal to T_0 at ground level and has a vertical gradient of $-0.01\ K/m$. At the top boundary, all quantities have *zero gradient* boundary conditions, except for $\vec{U}$ which has a fixed value corresponding to the free wind flow. On the bottom boundary, *no slip* condition has been used for $\vec{U}$ and wall functions for the turbulence parameters. The rest of the magnitudes have zero gradient conditions.

3.1. Simulation run

In a first step, the simulation is run for 100 s without exhaust gas to let the wind flow stabilize, the resulting velocity distribution is shown in Figure 3 a). In the upper part of the simulation domain the velocity field is parallel to the general wind flow. Closer to the ground, the wind flow is disturbed by the orography and the city buildings. In a second step, the simulation is run with the outflow from the exhaust included for at least 500 s so that the new air flow has reached a stationary regime. The atmospheric wind flow is now disturbed by the ascending air+CO_2 plume, see the Figure 3 b). The dynamic pressure, $P - \rho g z$, shows the low pressure zone created by the plume on the general air flow. CO_2 gas is transported upwards by the fast outgoing plume and subsequently is drifted following the general wind flow. At the same time, sidewards from the plume an outdiffusion of the pollutant happens. Part of it reaches the ground level where an excess of CO_2 can be built. The pollutant excess is defined as a 10% excess over the background level of $\sim 400\ ppm$. This happens mainly right below the plume but the width of the excess area, as well as, its downwind size is modified by the local orography and buildings, but also other factors. To study the influence of other factors a series of parameter studies have been performed.

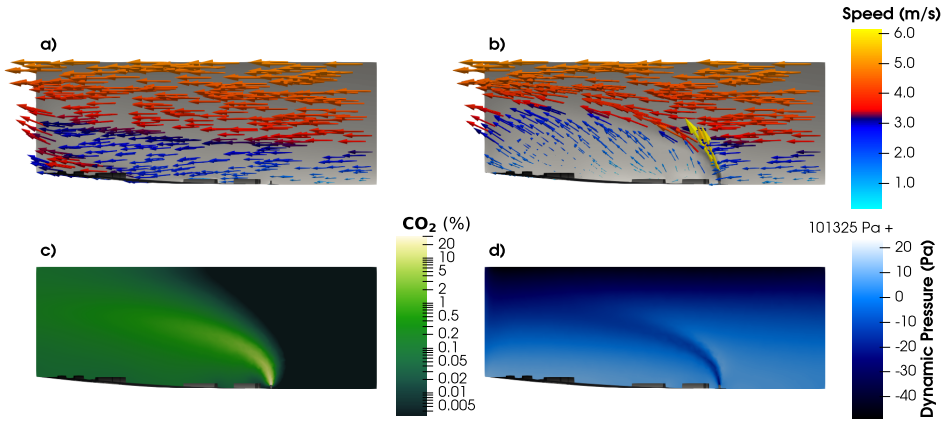

Figure 3. Simulation overview. Slice of the simulation domain parallel to the main wind flow, North-West $(-1, 1, 0)$, cut through the middle of the plume. The chimney is 10 m high, $T_0 = 10°C$, $T_c = 110°C$ and wind speed 5 m/s. The velocity values a) before the plume sets on and b) after. The c) concentration of CO_2 is given as percentages of the total mass. The d) dynamic pressure $P - \rho g z$ is also shown.

3.2. Wind direction

To study the concentration of CO_2 depending on the incoming wind direction, the direction of the wind has been modified for an incoming wind speed of 5 m/s. The chimney height has been kept 10 m high, the temperature of the plume $T_c = 110°\ c$ and the ambient temperature $10°C$.

Preprints (www.preprints.org) | NOT PEER-REVIEWED | Posted: 4 August 2021 doi:10.20944/preprints202108.0113.v1

The four chosen directions blow towards inland, approximately North-West or $(-1,1,0)$ wind, parallel to the coast, North-East or $(1,1,0)$ and South-West $(-1,-1,0)$ winds, and towards the sea, South-East $(1,-1,0)$ wind (see Figure 4).

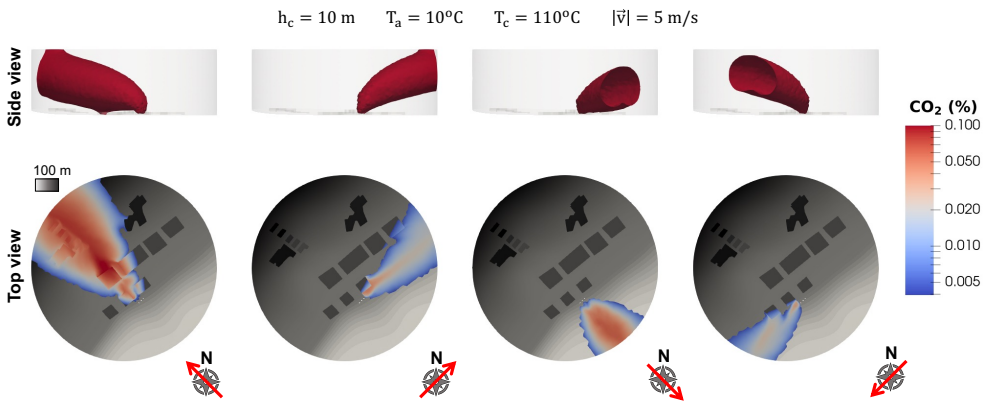

Figure 4. Wind direction. Concentration of CO_2 at ground level for wind speed $u = 5\ m/s$. The wind direction is represented by a red arrow. The chimney height is 10 m, the ambient temperature 10° and the exhaust gas temperature is 110°C in all cases. The terrain height has been represented in a grayscale. Lighter colors correspond to lower heights and the sea has the lightest color. The chimneys are three white spots near the coastline. The upper panels, show the concentration of CO_2 within the plume. The 0.1 %, 1000 ppm, surface for CO_2 has been plotted in all cases.

The concentration of CO_2 in the city only increases when the wind blows inland, North-West. The wind blowing in the opposite direction, towards the sea or South-East, also deposit pollutant gas on the sea. In both directions, the gentle slope of the terrain near the sea increases the deposition rate both inland and on the sea. In line with this, the wind blowing parallel to the coast, North-East and South-West, yield a much lower deposition of the pollutant. The main reason for this is that the exhaust plume travels upward higher.

3.3. Wind speed

The speed of the incoming flow is a determining factor in the range of dispersion of the pollutant. In general the largest concentration at ground level is always detected right below the plume. However, the sidewards distribution and the peak concentration value of the deposited gas molecules can vary remarkably. The widest distribution of excess pollutant is obtained for the lowest wind speed. Although the highest concentration is reached downwind, the concentration sideways remains high in the whole simulation domain. In addition, there is also a noticiable deposition of pollutant upwind. For a medium value, 5 m/s, and the highest value, 15 m/s, the gas deposition remains detectable in narrower areas. It has a width of $\sim$ 120 m in the first case and $\sim$ 200 m in the second at the maximum deposition concentration distance from the chimneys.

Preprints (www.preprints.org) | NOT PEER-REVIEWED | Posted: 4 August 2021 doi:10.20944/preprints202108.0113.v1

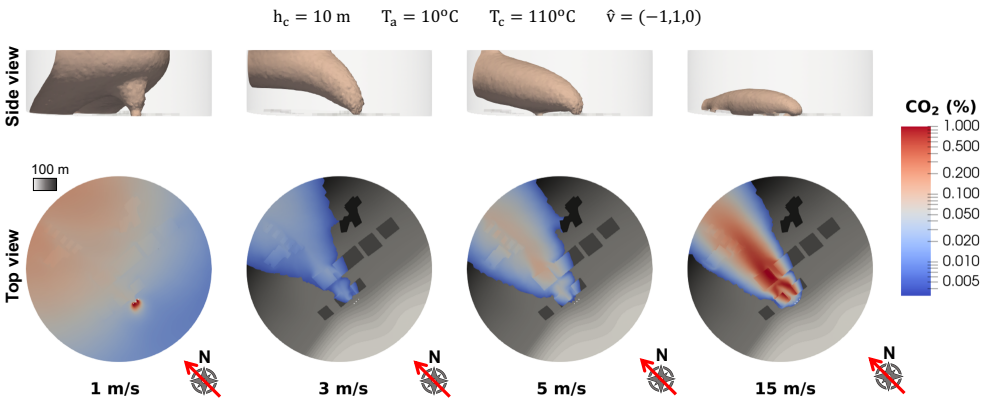

Figure 5. Wind speed. Concentration of CO_2 at ground level for inland North-West wind, $(-1,1,0)$. The chimney height is 10 m, the ambient temperature is $10°C$ and the exhaust gas temperature $110°C$ in all cases. The terrain height is represented in a grayscale. Lighter colors correspond to lower heights and the sea has the lightest color. The chimneys are three white spots near the coastline. The upper panels, show the CO_2 concentration isosurfaces (0.1 %, 1000 ppm) representing the plume distribution within the simulation domain.

The case with wind speed of 3 m/s is different from the rest in the fact that the deposition of pollutant is lower by an order of magnitude. This anomaly is better understood by noting that the plume, see side view of Figure 5, flows higher and therefore less pollutant reach the ground. Larger wind speeds increase the drag of the gas molecules away from the chimney diminishing the time for lateral dispersion. This effect is the main reason why the concentration of pollutant is radically smaller when going from wind speeds of 1 m/s to 3 m/s. At larger wind speeds, the maximum height reached by the plume is shortened by the stronger pull exerted by the main wind flow. The interplay between these factors, being the first dominant for low wind speeds and the later for wind speeds above 5 m/s, explains the observed trend.

3.4. Temperature of the plume

Another important factor determining the final distribution of CO_2 in the ground is the temperature of the outflowing gas at the chimney exit. Higher outflow temperature enhances the upwards buoyancy of the exhaust gas due to its lower density. Contrarily, at lower temperatures the exhaust gas will get dragged downwards. When the temperature of the exhaust gas is equal to the ambient temperature $T_c = 10°C$, see Figure 6, the amount of deposited pollutant is strongly enhanced. When the exhaust gas temperature is $T_c = 210°C$ the concentration decreases by 2 orders of magnitude and the side range of the deposited gas decreases to less than half.

Preprints (www.preprints.org) | NOT PEER-REVIEWED | Posted: 4 August 2021 doi:10.20944/preprints202108.0113.v1

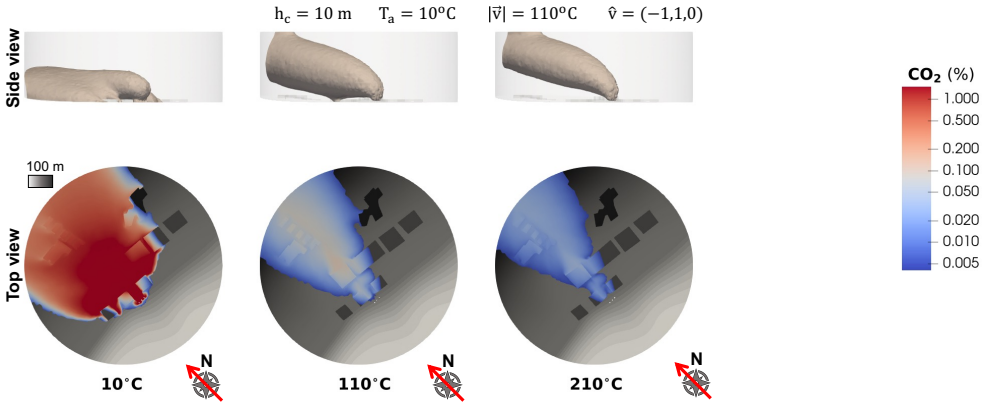

Figure 6. Exhaust gas Temperature. Concentration of CO_2 at ground level for wind speed $u = 5\ m/s$ and North-West $(-1, 1, 0)$ direction. The chimney height is 10 m and the ambient temperature $10°C$ in all cases. The terrain height is represented in a grayscale. Lighter colors correspond to lower heights and the sea has the lightest color. The chimneys are three white spots near the coastline. The upper panels, show the concentration of CO_2 within the plume. The 0.1 %, 1000 ppm, surface for CO_2 has been plotted in all cases.

3.5. Chimney height

The chimney height (see Figure 7) has a negligible effect on the deposited gas within the simulated area. Also the ambient temperature, shown in Figure 8, has a small effect on the deposited pollutant. In all cases, the region where a significant deposition of CO_2 is observed remains largely unchanged and the concentration of the deposited pollutant is also similar.

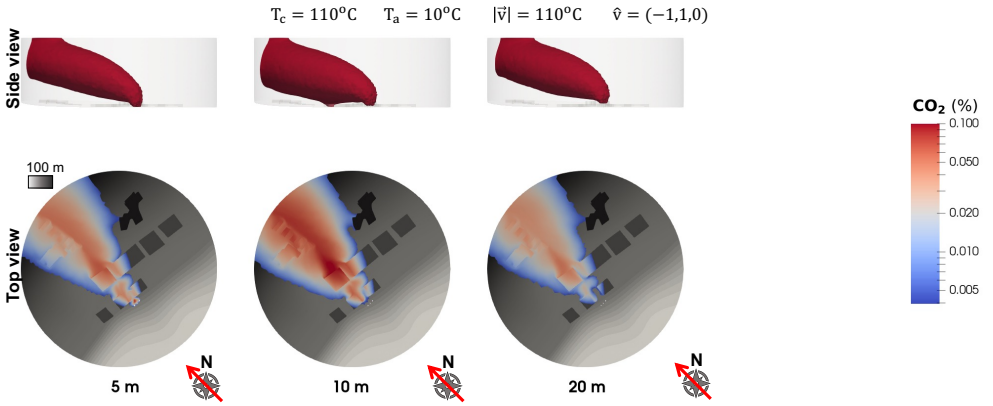

Figure 7. Chimney height. Concentration of CO_2 at ground level for wind speed $u = 5\ m/s$ and North-West $(-1, 1, 0)$ direction. The concentration values have been given as a percentage of the gas particles (10^4 ppm). The ambient temperature is $10°C$ and the exhaust gas temperature $110°C$ in all cases. The terrain height is represented in a grayscale. Lighter colors correspond to lower heights and the sea has the lightest color. The chimneys are three white spots near the coastline. The upper panels, show the concentration of CO_2 within the plume. The 0.1 %, 1000 ppm, surface for CO_2 has been plotted in all cases.

Preprints (www.preprints.org) | NOT PEER-REVIEWED | Posted: 4 August 2021 doi:10.20944/preprints202108.0113.v1

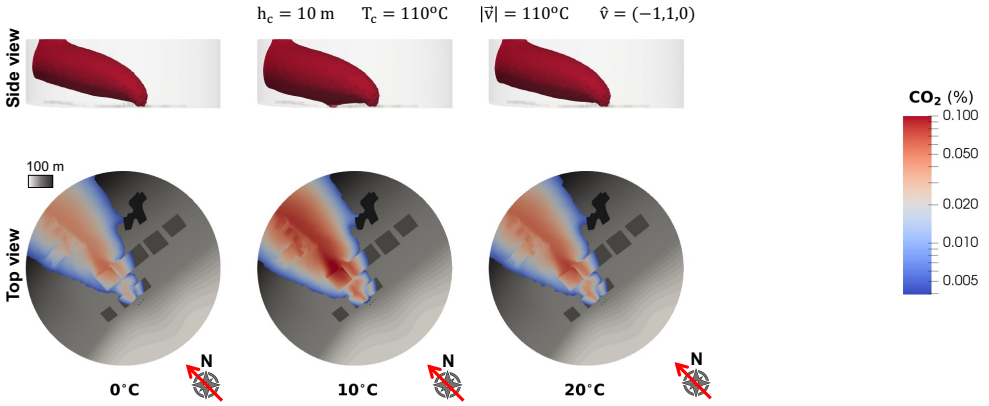

Figure 8. Ambient Temperature. Concentration of CO_2 at ground level for wind speed $u = 5\ m/s$ and North-West $(-1,1,0)$ direction. The chimney height is 10 m and the exhaust gas temperature $110°C$ in all cases. The terrain height is represented in a grayscale. Lighter colors correspond to lower heights and the sea has the lightest color. The chimneys are three white spots near the coastline. The upper panels, show the concentration of CO_2 within the plume. The 0.1 %, 1000 ppm, surface for CO_2 has been plotted in all cases.

4. Discussion

The wind blowing directly inland, North-West $(-1,1,0)$, is found to be the most relevant to understand the transport of gas phase pollutants into the city. In all cases, the deposition of CO_2 is the largest right below the center of the plume. When the wind speed is very low the concentration downwind stays relatively constant within the simulated domain, as can be seen in Figure 9. The drag of the main wind flow is low and the pollutant disperses mostly by diffusion. It must be noted that the concentration upwind has a sharp maximum near the chimney and decays fast at larger distances as shown in Figure 5. For slightly larger wind speeds, the deposited gas increases up to a distance of around 200 m. At longer distances it remains roughly constant until the boundary of the simulation domain. When the wind speed is 5 m/s or higher, the pollutant still has a peak concentration, but at longer distances from the chimney, the concentration of pollutant decreases, specially for the largest wind flow speed. The peak CO_2 concentration is the lowest at moderate speeds 3 m/s and it increases steadily as the wind speed increases.

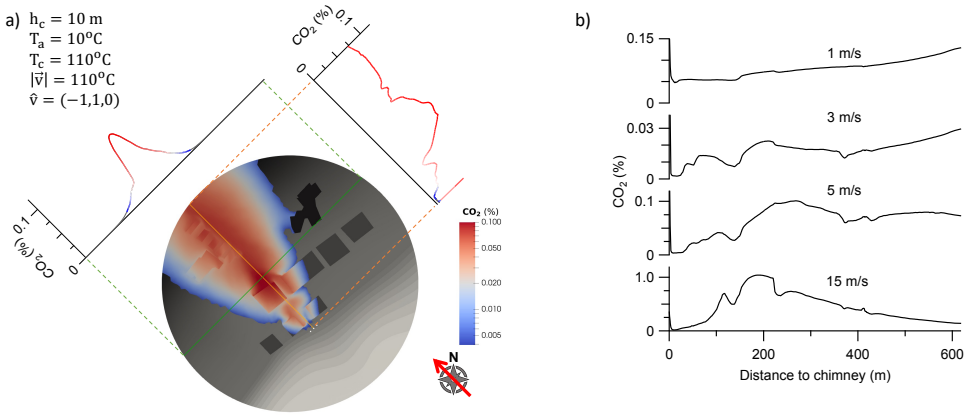

Figure 9. CO_2 concentration sections. The left panel shows the line distribution of CO_2 parallel to the main wind flow of 5 m/s (orange line) below the center of the plume where the concentration is the highest. A line distribution crossing the plume perpendicular to the wind flow along the highest concentration (green line) is also shown. The right panel shows the CO_2 distribution downwind for 1, 3, 5 and 15 m/s wind speeds. The wind blows in the North-West $(-1,1,0)$ direction. The chimney is 10 m high and the gas has $110°C$ at the exit of the plume. The ambient temperature is $10°C$.

 doi:10.20944/preprints202108.0113.v1

The lateral distribution is the widest at very low speed due to the weak drag. At moderate speeds decreases sharply due to the low deposition rate and at speeds of 5 m/s it takes a triangular shape and a size that remains largely unchanged. The wind speed, chimney height, plume temperature and ambient temperature has little effect in the lateral width of the deposition range. The wind direction has a larger influence mainly due to the local disturbance of the general wind flow driven by the orography and the city buildings. Winds with a downhill or uphill directions are seen to provoke a larger deposition of gas pollutants. On the other hand, for winds blowing the plume in flat regions, the upwards buoyancy effect get enhanced by the wind flow largely parallel to the ground.

Inside the city localized pockets with high concentration of pollutants can be created which can have a negative influence in the air quality. An example can be seen in the third and fourth panels of Figure 5. This effect is more apparent close to the emission point, or around 200 m for the conditions of this work. Another important factor is the plume temperature. The deposition is enhanced when the plume has a temperature close to the ambient temperature, what can have technological implications when low emission temperatures reflect lower working temperature conditions of the engine of the vessel. Engines working at lower temperature can increase its energy efficiency, but the impact of the pollutants expelled in the plume is larger in the surrounding areas. Therefore, it would require a more careful treatment of the exhaust gas.

A point that future works need to address is the effect of other pollutant gases than CO_2. Given that pollutants tend to have a larger molecular mass than clean air, their distribution are expected to mirror the distribution of CO_2, which also has larger molecular mass. The general trends observed for CO_2 should also be valid for other pollutants. However, the typical concentration of pollutants at the emission point is normally lower than assumed in this work. This will decrease the peak deposited amount of pollutant and it can decrease the lateral range of the deposited pollutant. A detailed discussion of the effects of other pollutants and, specially, particulate matter would require a follow-up work where the composition of the exhaust gas is varied. The simulation domain should also be enlarged downwind to find the deposition range along the wind axis direction. In like manner, studying the deposition of particulate matter would require a longer simulation domain downwind.

5. Conclusions

An accurate CFD model of the harbour area of Tromsø has been built in order to model the deposition of CO_2 gas emitted by docked vessels within the city. It includes buoyancy and fluid compressibility effects as well as the thermodynamics of perfect gases. The stabilization of the general wind flow has been achieved by forcing the atmospheric boundary layer conditions in the lateral boundaries of the domain. The diffusion of CO_2 out of the plume into the surrounding air is also modelled and it is found to have noticeable effects, specially at low wind speeds. The influence of the wind speed and direction, vessel chimney height, ambient temperature and exhaust gas temperature have been studied. The wind direction, as expected, determines the direction where the pollutant gas will be deposited. More interesting is the trend found when varying the wind speed blowing inland. The deposition range is the largest when the wind speed is very low. In this case the diffusion effects dominate over the transport effects and the pollutant gas has a wide distribution range extending several hundred meters downwind and in lateral direction. At moderate speeds, the plume is transported far from the city area before the deposition happens. Interestingly, at even larger speeds, the height of the plume is shortened increasing the deposition below the plume. The lateral distribution is $100 - 200$ m wide in most cases. The simulations show that the interplay between the main wind flow, the local orography and the city buildings can create pockets of high pollutant concentration.

This simulation model can be extended to study other type of pollutants or particulate matter. They can be of high interest for the detailed study of the contamination in cities

near the coast or an industrial pollutant source. A next step to increase the accuracy of this model would be the validation of the results using field data.

Author Contributions: For research articles with several authors, a short paragraph specifying their individual contributions must be provided. The following statements should be used "Conceptualization, A.Z. H.K. and G.B.; methodology, A.Z.; software, A.Z.; formal analysis, A.Z.; investigation, A.Z.; resources, S.M.; data curation, S.M.; writing—original draft preparation, A.Z.; writing—review and editing, A.Z., S.M., H.K. and G.B.; visualization, A.Z.; project administration, H.K. and G.B.; funding acquisition, H.K. and G.B. All authors have read and agreed to the published version of the manuscript.", please turn to the CRediT taxonomy for the term explanation. Authorship must be limited to those who have contributed substantially to the work reported.

Funding: This research received no external funding. The APC was funded by the Zurich University of Applied Sciences (ZHAW).

Conflicts of Interest: The authors declare no conflict of interest. The funders had no role in the design of the study; in the collection, analyses, or interpretation of data; in the writing of the manuscript, or in the decision to publish the results

References

1. Kim, K.H.; Kabir, E.; Kabir, S. A review on the human health impact of airborne particulate matter. *Environment International* **2015**, *74*, 136–143. doi:10.1016/j.envint.2014.10.005.
2. Davidson, C.I.; Phalen, R.F.; Solomon, P.A. Airborne Particulate Matter and Human Health: A Review. *Aerosol Science and Technology* **2005**, *39*, 737–749. doi:10.1080/02786820500191348.
3. Roskilly, A.P.; Nanda, S.K.; Wang, Y.D.; Chirkowski, J. The performance and the gaseous emissions of two small marine craft diesel engines fuelled with biodiesel. *Applied Thermal Engineering* **2008**, *28*, 872–880. doi:10.1016/j.applthermaleng.2007.07.007.
4. Walter, R.A.; Broderick, A.J.; Sturm, J.C.; Klaubert, E.C. USCG Pollution Abatement Program : A Preliminary Study of Vessel and Boat Exhaust Emissions **1971**.
5. Simeone, L.F. The intrusion of engine exhaust into the passenger areas of recreational power boats **1991**.
6. Bentz, A.P.; Weaver, E. Marine Diesel Exhaust Emissions Measured by Portable Instruments. *SAE Transactions* **1994**, *103*, 1872–1876. Publisher: SAE International.
7. Johansson, L.; Ytreberg, E.; Jalkanen, J.P.; Fridell, E.; Eriksson, K.M.; Lagerström, M.; Maljutenko, I.; Raudsepp, U.; Fischer, V.; Roth, E. Model for leisure boat activities and emissions – implementation for the Baltic Sea. *Ocean Science* **2020**, *16*, 1143–1163. Publisher: Copernicus GmbH, doi:10.5194/os-16-1143-2020.
8. H. M. A. Schleijpen.; Filip P. Neele. Ship exhaust gas plume cooling. Targets and Backgrounds X: Characterization and Representation, 2004, Vol. 5431.
9. Garcia-Gonzales, D.A.; Shamasunder, B.; Jerrett, M. Distance decay gradients in hazardous air pollution concentrations around oil and natural gas facilities in the city of Los Angeles: A pilot study. *Environmental Research* **2019**, *173*, 232–236. doi:10.1016/j.envres.2019.03.027.
10. Ran, L.; Lin, W.L.; Deji, Y.Z.; La, B.; Tsering, P.M.; Xu, X.B.; Wang, W. Surface gas pollutants in Lhasa, a highland city of Tibet; current levels and pollution implications. *Atmospheric Chemistry and Physics* **2014**, *14*, 10721–10730. Publisher: Copernicus GmbH, doi:10.5194/acp-14-10721-2014.
11. Zhang, R.; Wang, G.; Guo, S.; Zamora, M.L.; Ying, Q.; Lin, Y.; Wang, W.; Hu, M.; Wang, Y. Formation of Urban Fine Particulate Matter. *Chemical Reviews* **2015**, *115*, 3803–3855. Publisher: American Chemical Society, doi:10.1021/acs.chemrev.5b00067.
12. Launder, B.E.; Spalding, D.B. The numerical computation of turbulent flows. *Computer Methods in Applied Mechanics and Engineering* **1974**, *3*, 269–289. doi:10.1016/0045-7825(74)90029-2.
13. Richards, P.J.; Hoxey, R.P. Appropriate boundary conditions for computational wind engineering models using the k-ϵ turbulence model. *Journal of Wind Engineering and Industrial Aerodynamics* **1993**, *46-47*, 145–153. doi:10.1016/0167-6105(93)90124-7.
14. Hargreaves, D.M.; Wright, N.G. On the use of the k–ϵ model in commercial CFD software to model the neutral atmospheric boundary layer. *Journal of Wind Engineering and Industrial Aerodynamics* **2007**, *95*, 355–369. doi:10.1016/j.jweia.2006.08.002.
15. Yang, Y.; Gu, M.; Chen, S.; Jin, X. New inflow boundary conditions for modelling the neutral equilibrium atmospheric boundary layer in computational wind engineering. *Journal of Wind Engineering and Industrial Aerodynamics* **2009**, *97*, 88–95. doi:10.1016/j.jweia.2008.12.001.
16. Weller, H.G.; Tabor, G.; Jasak, H.; Fureby, C. A tensorial approach to computational continuum mechanics using object-oriented techniques. *Computers in Physics* **1998**, *12*, 620–631. Publisher: American Institute of Physics, doi:10.1063/1.168744.
17. Issa, R.I. Solution of the implicitly discretised fluid flow equations by operator-splitting. *Journal of Computational Physics* **1986**, *62*, 40–65. doi:10.1016/0021-9991(86)90099-9.
18. Caretto, L.S.; Gosman, A.D.; Patankar, S.V.; Spalding, D.B. Two calculation procedures for steady, three-dimensional flows with recirculation. Proceedings of the Third International Conference on Numerical Methods in Fluid Mechanics; Cabannes, H.; Temam, R., Eds.; Springer: Berlin, Heidelberg, 1973; Lecture Notes in Physics, pp. 60–68. doi:10.1007/BFb0112677.

19. Garratt, J.R. Review: the atmospheric boundary layer. *Earth-Science Reviews* **1994**, *37*, 89–134. doi:10.1016/0012-8252(94)90026-4.
20. Tran, V.; Ng, E.Y.K.; Skote, M. CFD simulation of dense gas dispersion in neutral atmospheric boundary layer with OpenFOAM. *Meteorology and Atmospheric Physics* **2019**. doi:10.1007/s00703-019-00689-2.
21. Richards, P.J.; Norris, S.E. Appropriate boundary conditions for computational wind engineering models revisited. *Journal of Wind Engineering and Industrial Aerodynamics* **2011**, *99*, 257–266. doi:10.1016/j.jweia.2010.12.008.